13th World Conference on Earthquake Engineering
Vancouver, B.C., Canada
August 1-6, 2004
Paper No. 2397

DEFORMATION INDICES FOR CONCRETE COLUMNS: PREDICTED VS. MEASURED

M. Inel[1], M. Aschheim[2], and S. Pantazopoulou[3]

SUMMARY

The transition to displacement-controlled methods for seismic design rely explicitly on measures of deformation capacity. Although conceptually clearly defined, the various alternative indices such as displacement ductility, drift, and plastic rotation capacity calculated with the available analytical tools in the literature are marked by excessive scatter when tested with well controlled experimental results, indicating that the validity of the underlying physical models is questionable. This problem is explored systematically in the paper, by evaluating the parametric performance of the analytical models, as well as though comparison with the experimental trends. An important result of the study is that well confined members designed as per the ATC-32 requirements have large dependable deformation capacities regardless of the axial load ratio, a finding with significant implications in practical bridge seismic design.

INTRODUCTION

A fundamental objective in the seismic design of structures capable of inelastic response is to ensure that the deformation capacities of the structure and its components exceed the associated deformation demands. This objective is addressed implicitly in capacity-based procedures, and is an explicit core requirement of displacement-based design procedures. For the design of bridge structures, the deformation capacities of reinforced concrete columns are of particular interest, because the columns (or piers) typically are the preferred locations of inelastic behavior for these systems.

Quantification of the dependable deformation capacity of bridge columns is essential for the development of a framework for the displacement-based design of bridges. A variety of indices of deformability may be

[1] Assistant Professor, Department of Civil Engineering, Pamukkale University, Denizli, Turkey 20017; minel@pamukkale.edu.tr.
[2] Associate Professor, Department of Civil Engineering, Santa Clara University, 500 El Camino Real, Santa Clara, CA 95050; maschheim@scu.edu.
[3] Professor, Department of Civil Engineering, Demokritus University, Xanthi, Greece 67100; pantaz@civil.duth.gr.

prescribed, at the scale of the member, hinge, cross section, or fiber. These include the drift and displacement ductility associated with displacement at the top of the column, plastic hinge rotation, curvature ductility, and the strain and strain ductility associated with fibers of the critical cross section. Target values of these indices may be associated with different limit states, ranging from yield to ultimate.

Methods for estimating the deformation capacity of reinforced concrete columns have been the focus of many research studies. Several available models for estimating column deformation capacity include those by Park [1], Priestley [2], Lehman [3], Elwood [4], and Fardis [5]. The models presented in Fardis [5] represent a significant extension of the work begun by Panagiotakos [6]. Except for the empirical models of Elwood [4] and Fardis [5], these models estimate the deformation capacity at yielding and ultimate based on lumped plasticity idealization for a cantilever, as shown in Figure 1. The simplest form of such model is to compute deformation capacities based on flexural contributions, assuming the curvature distributions of Figure 1, as described by Park [1]. This approach is termed the "simple" model in this paper.

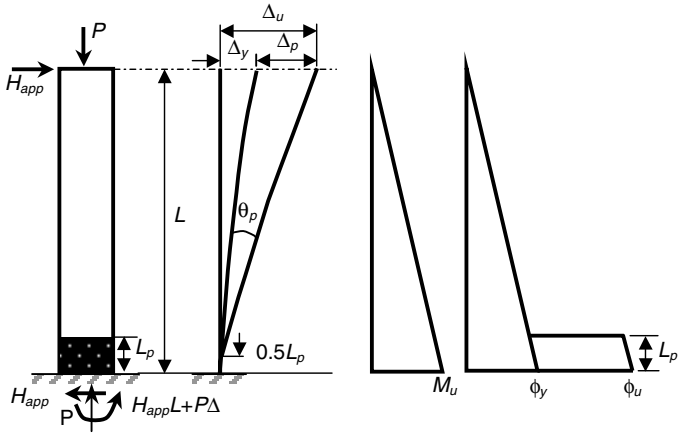

Figure 1. Lumped plasticity model for a cantilever column

Elwood [4] proposed empirical models to estimate drift capacities of reinforced concrete columns at shear and axial load failures. He also developed an elaborate computer model whereby the plastic hinge region was modeled by a series of a rotational, a sideways translational and a longitudinal spring in order to represent the combined inelasticity resulting from flexure shear and axial compression in a typical column during lateral sway. In Fardis [5], expressions were developed for members under cyclic loading ultimately failing in shear after initially yielding in flexure. The other models are intended for estimating the deformation capacities of members whose behavior is dominated by flexural deformations. Available models for estimating deformation capacities are reviewed in this study in an attempt to characterize the model predictions and to establish the parametric sensitivity of various indices of deformation capacity. A limited set of experimental data obtained from tests of large-scale reinforced concrete columns having rectangular cross sections is also considered. All columns of the experimental data set have sufficient shear strength according to the shear strength equations of ATC-32 [7] that a shear failure would not be expected to occur, even after flexural hinging develops. Therefore, the Elwood [4] model and the portions of the Fardis [5] model related to pre-emptive shear failure are not considered further. Estimates of the deformation capacities of the columns obtained from the five models are compared with the observed values. It is found that nominal deformation capacities for columns with reinforcement per ATC-32 may be recommended that are independent of the axial load ratio based on the experimental data.

EVALUATION OF INELASTIC DEFORMATION CAPACITIES

The load-deformation behavior of a column is commonly idealized by a bilinear curve that is fit to the analytic response estimate or that may be fitted approximately to the envelope of experimental load-deformation response. The bilinear curve may be defined by two points, the yield and ultimate displacements (Δ_y and Δ_u) and the corresponding loads, although various definitions of these points have been used by different researchers. Once the yield and ultimate points are established, the displacement ductility, μ_δ, plastic displacement, Δ_p, plastic hinge rotation, θ_p, and peak drift, δ_d capacities may be derived for the cantilever column of Figure 1.

$$\mu_\delta = \frac{\Delta_u}{\Delta_y} \tag{1}$$

$$\Delta_p = \Delta_u - \Delta_y \tag{2}$$

$$\theta_p = \frac{\Delta_u - \Delta_y}{L - 0.5L_p} \tag{3}$$

$$\delta_d = \frac{\Delta_u}{L} \tag{4}$$

Whereas the experimental data is invaluable, the design of columns normally relies on calculated estimates of the load-deformation behavior, as illustrated in Figure 2. The yield and ultimate displacements may be estimated by including the contributions of flexure, shear, and anchorage slip, as proposed by various researchers.

$$\Delta_y = \Delta_{y,flexure} + \Delta_{y,slip} + \Delta_{y,shear} \tag{5}$$

$$\Delta_u = \Delta_{u,flexure} + \Delta_{u,slip} + \Delta_{u,shear} \tag{6}$$

The five models considered in this paper are: (1) the so-called "simple" model, (2) the model by Lehman (Lehman [3]), (3) the analytical model by Fardis (Fardis [5]), (4) the empirical model by Fardis (Fardis [5]), and (5) the model by Priestley (Priestley [2]). The calculation procedure for yield and ultimate displacements according to the five models is summarized in Table 1.

Development and calibration of the models requires that contributions to deformation be partitioned to the various components that are represented explicitly in each analytical model. Except for the Fardis empirical model, yield and ultimate curvatures must be calculated. At the ultimate point, those models that explicitly include displacements due to shear and anchorage slip do so by lumping these contributions into the plastic hinge length. Since in most cases, the proposed plastic hinge lengths are based on numerical calculations to reproduce experimentally determined displacements at flexural yield and ultimate, the plastic hinge length used by the investigators cannot be considered independently of the definitions of yield and ultimate curvatures. The Fardis analytical model provides explicit expressions for the calculation of yield and ultimate curvatures. In this paper, the Mander model for confinement (Mander [8]) is implemented in the moment-curvature analyses required for the "simple", Lehman, and Priestley models. The definition of ultimate curvature depends on ultimate strain; we impose additional constraints on definition of ultimate strain described below (i.e. steel strain and 0.8Mmax).

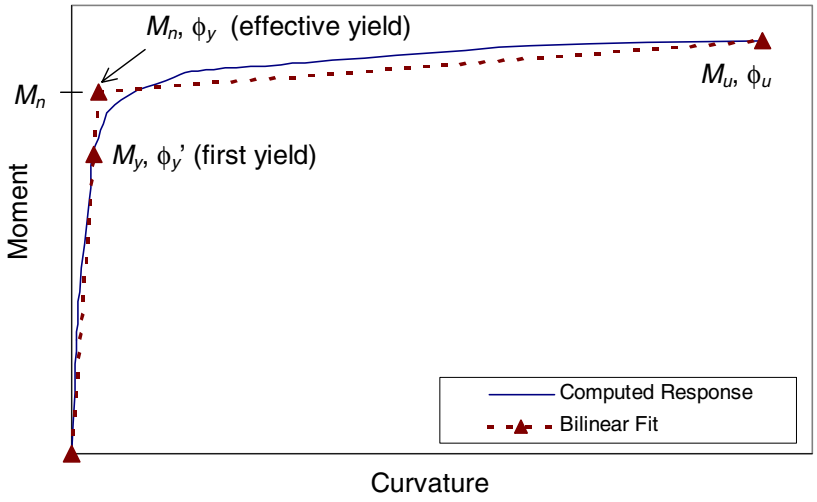

Figure 2. Typical moment-curvature response of a well-confined column

Table 1. Definition of deformation indices using available models

Deformation Index	"Simple" Model	Lehman Model	Fardis Analytical Model	Fardis Empirical Model	Priestley Model
$\Delta_{y,flexure}$	$\phi_y L^2/3$	$\phi_y L^2/3$	$\phi_y L^2/3$	$\phi_y L^2/3$	$\phi_y(L+0.15f_y d_b)^2/3$
$\Delta_{y,shear}$	NA	$V_y L/(0.4E_{c,sec}0.8A_g)$	0.00275L	0.00275L	$\Delta_{conc,\ shear}+\Delta_{truss,\ shear}$ [1]
$\Delta_{y,slip}$	NA	$\phi_y L f_y d_b/8vf_c$'	$\varepsilon_y f_y d_b L/(5f_c'(d-d'))$	$\varepsilon_y f_y d_b L/(5f_c'(d-d'))$	Included in $\Delta_{y,flexure}$
θ_p	$(\phi_u-\phi_y)L_p$	$(\phi_u-\phi_y)L_p$	$(\phi_u-\phi_y)Lp$ [2]	$\theta_u-\Delta_y/L$	$(\phi_u-\phi_y)L_p$
θ_u	Δ_u/L	Δ_u/L	Δ_u/L	[2]	Δ_u/L
Δ_p	$\theta_p(L-0.5\ L_p)$	$\theta_p(L-0.5\ L_p)$	$\theta_p(L-0.5\ L_p)$	$\Delta_u-\Delta_y$	$\theta_p(L-0.5\ L_p)$
Δ_u	$\Delta_y+\Delta_p$	$\Delta_y+\Delta_p$	$\Delta_y+\Delta_p$	$\theta_u L$	$\Delta_y+\Delta_p$
L_p	0.5H	$0.5L(M_u-M_n)/M_n$ $+1.2(f_u-f_y)\ d_b/4vf_c$'	$0.026L+0.13H$ $+0.02f_y d_b$	NA	$0.08L+0.022f_y d_b$

NA: Not Applicable

[1] Details for shear contribution to yield displacement can be found in Priestley [2]

[2] Details for Fardis analytical and empirical models can be found in Panagiotakos [6] and Fardis [5].

Figure 2 shows the moment-curvature response computed for a typical well-confined column. The dashed curve is a bilinear curve fitted to the computed curve. The bilinear curve is defined by an effective yield point (M_n, ϕ_y) and by a nominal point of failure of the cross-section (M_u, ϕ_u). The "yield" point (M_y, ϕ_y') is defined as the point when the extreme tension steel yields or the strain in the concrete at the extreme compression fiber reaches 0.002, whichever comes first, a definition used by others (e.g. Priestley [2, 9]). For any axial load level, the nominal flexural strength, M_n, is calculated using a rectangular stress block. The specified yield and compressive strengths were used without reduction factors in the analytical study. Similarly, the reported yield and compressive strengths were used without reduction factors to assess the experimental data. For the analytical study the ultimate curvature is defined as the smallest of the curvatures corresponding to (1) a reduced moment equal to 20% of maximum moment, determined from the moment-curvature analysis, (2) the extreme compression fiber reaching the ultimate concrete compressive strain as determined using the Mander model, and (3) the longitudinal steel reaching a tensile strain of 50% of ultimate strain capacity.

Inelastic Deformation Capacities from Analytical Models

Using the five models, the sensitivity of the inelastic deformation capacities was studied for cantilevered columns by varying cross section size, aspect ratio, transverse reinforcement amount, and axial load ratio. In one set of analyses, three cross section sizes (305 mm x 305mm, 610 mm x 610 mm, 1220 mm x 1220 mm) were used, with the aspect ratio (cantilever length divided by section depth) held constant at 4. In a second set of analyses, aspect ratios were changed from 2 to 10 by varying the column length while the cross section was kept constant. Two levels of transverse reinforcement were considered: the amount required per ATC-32 [7] recommendations and one tenth of the ATC-32 requirement, termed in the remainder of this paper as "well-confined" and "poorly-confined", respectively. The ATC-32 transverse reinforcement requirements are provided in the Appendix. Two levels of axial load were considered, equal to 0.1 and 0.5 times $A_g f_c'$. Material properties were constant for the cases considered; 420 MPa yield strength for both longitudinal and transverse steel and 27.5 MPa for concrete. The longitudinal reinforcement ratio was 1.5% for all cases.

Neglecting minor differences due to cover requirements, the displacement ductility, plastic hinge rotation, and ultimate drift capacities predicted by the deformation capacity models were independent of the cross section size under the constraint of constant aspect ratio of 4. Figures 3, 4, and 5 shows how the calculated displacement ductility, plastic hinge rotation and peak drift measurements change with aspect ratio for an invariant cross section, respectively. The figure also illustrates the effect of the transverse steel amount, axial load ratio, and the influence of the model used to estimate deformation capacity. Details are available in Inel [10]. The overall trends exhibited by the collection of models lead to the following observations: (a) except for the plastic hinge rotation capacity estimated by the "simple" model, no parameter is invariant with changes in aspect ratio, (b) the sensitivity of the inelastic deformation quantities to the models is obvious; different models can result in substantially different estimates of deformation capacity, (c) the effect of axial load ratio on deformation capacity is clear for the poorly-confined case; deformation capacities are smaller for the high axial load case, even though the ATC-32 compliant transverse steel is greater than for the case of low axial load ratio, and (d) well-confined columns can exhibit substantial calculated deformation capacities, for the cases investigated (axial loads equal to 0.1 and 0.5 times $A_g f_c'$).

Differences in deformation capacities estimated with the models are greater for the high axial load ratio case. The largest differences are observed in the plastic hinge rotation and drift capacities for high aspect ratios, while the largest differences in the displacement ductility capacity are observed for low aspect ratios (Inel, [9]). Key observations related to the individual models are: (a) the "simple" model tends to provide a lower bound estimate of plastic hinge rotation and peak drift for the well-confined case, (b) the Lehman model is sensitive to the level of confinement. For the poorly-confined case, the deformation capacities estimated by the Lehman model are considerably smaller than those estimated by the Priestley model for the low axial load ratio case, (c) the Lehman model is sensitive to the level of axial load. For the well-confined columns with high axial load ratio, plastic hinge rotation and drift capacities estimated by the Lehman model are considerably higher than those estimated by the other models. The reason for this seems to be that the plastic hinge length suggested by Lehman [3] depends explicitly on the axial load ratio while the other models have plastic hinge lengths that are independent of the axial load ratio. For example, for the well-confined case with aspect ratio of 4, when the axial load ratio increases from 0.1 to 0.5, the plastic hinge length estimated by the Lehman model almost doubles. It should also be noted that although no limitations are identified in the use of the model, Lehman proposed the plastic hinge length equation based on test data for the axial load ratio of 0.1, (d) for the Fardis analytical model, the displacement ductility capacities are nearly independent of the aspect ratio. This contradicts the generally accepted (and experimentally verified by Lehman [3]) trend that displacement ductility capacity decreases as aspect ratio increases. One reason this occurs is that the plastic hinge lengths, estimated by the Fardis analytical model, are considerably smaller for small aspect ratios than those determined by other models

such as the Priestley model. Another reason is that the shear displacement contribution to the yield displacement for the Fardis analytical model can be substantial (e.g., the shear contribution may exceed the flexural contribution for an aspect ratio of 2, depending on the axial load ratio), resulting in larger yield displacements. The combination of smaller ultimate displacement capacity and larger yield displacements for small aspect ratios results in smaller ductility capacities; this leads to results counter to the expected trend in displacement ductility capacity as a function of aspect ratio, and (e) the Fardis empirical model tends to estimate higher displacement ductility, plastic hinge rotation, and peak drift capacities than the other models for the poorly-confined case.

In summary, the sensitivity study indicates that none of the inelastic deformation capacity parameters (plastic hinge rotation, displacement ductility, and peak drift capacities) are a robust, invariant measure of inelastic deformation capacity, for the cases of varying aspect ratio considered. Because of the large range in deformation capacities predicted by the various analytical models, a limited amount of experimental data was considered to better understand the predictive capability of these models and to discern whether the experimental data might suggest a robust parameter for evaluating deformation capacity.

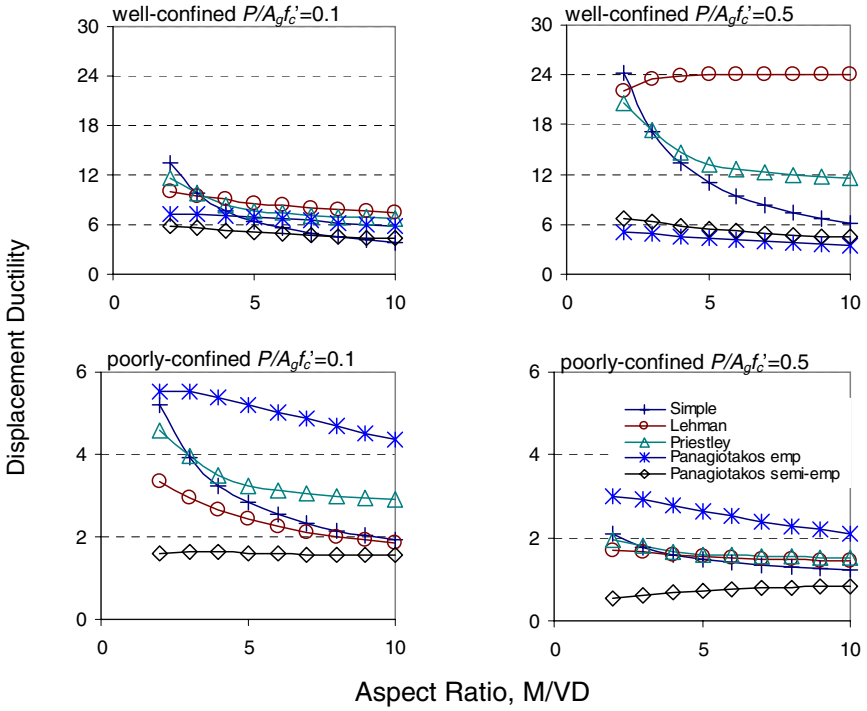

Figure 3. The effect of change in aspect ratio on the displacement ductility measurement quantities computed using the different models.

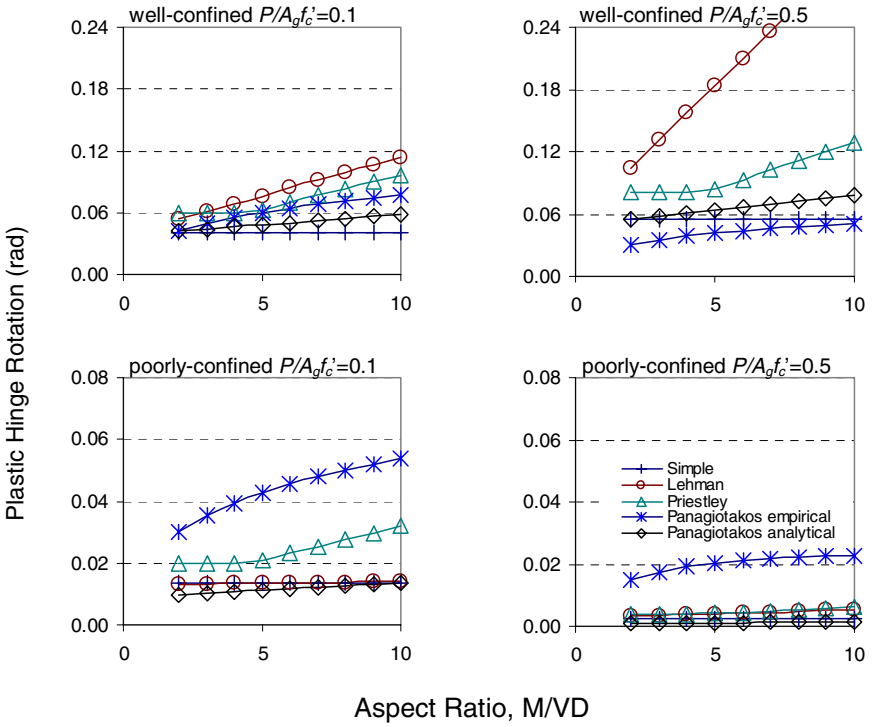

Figure 4. The effect of change in aspect ratio on the plastic hinge rotation measurement quantities computed using the different models.

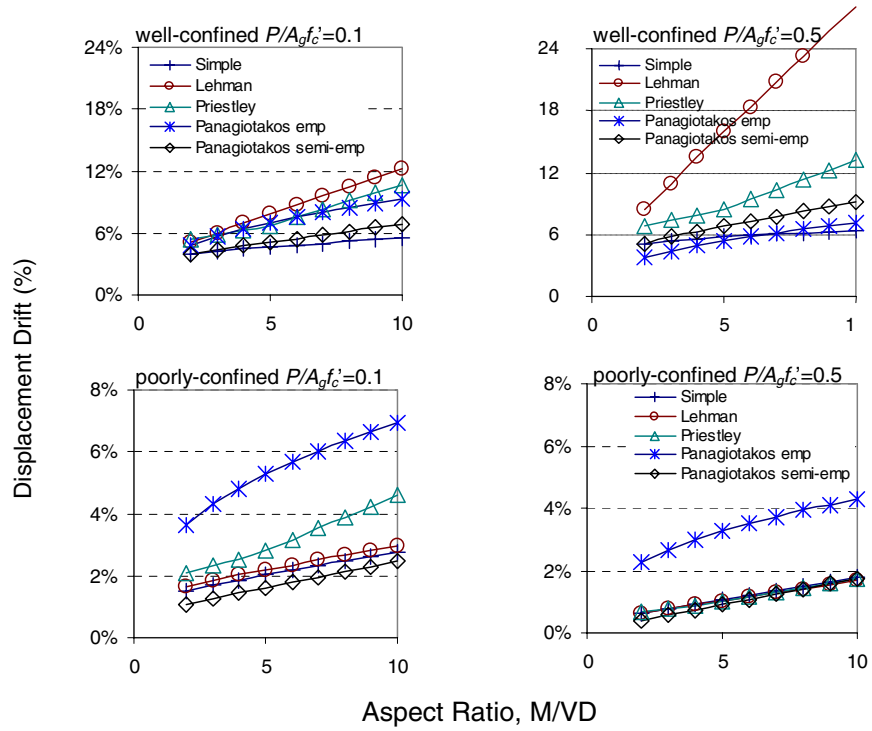

Figure 5. The effect of change in aspect ratio on the peak drift measurement quantities computed using the different models.

Inelastic Deformation Capacities from Experimental Data Set

The experimental data considered here was obtained from large-scale tests of rectangular reinforced concrete columns subjected to quasi-static reversed cyclic lateral loading, with axial load ratios of varied intensities held constant throughout the tests. Criteria used to establish the database were: (1) a rectangular cross section with minimum dimension of 300 mm, (2) at least 8 longitudinal bars, each laterally supported by transverse reinforcement, and (3) minimum aspect ratio (M/VD) of 2.5. A total of 23 tests with information required were retained among a total of 29 specimens conforming to these criteria. The retained specimens had square cross sections, aspect ratios ranging from 2.86 to 4.83, axial load ratios, $P/f_c'A_g$, ranging between 0.10 and 0.77, f_c' between 22 and 47 MPa, longitudinal reinforcement ratios ranged between 1.5 and 3.3% of the gross sectional area with yield strength of 430 to 510 MPa. Table 2 lists important descriptive parameters of the retained specimens.

Experimental data was evaluated by identifying an envelope of the moment at the base of column that includes the applied (actuator) force-deformation plot and the P-Δ contribution arising from the applied axial load. That is, $M = H_{app}L + P\Delta$, where H_{app}= applied horizontal force, P= applied axial load, and L is column height. It should be noted that secondary moment caused by P-δ along the length of member is neglected. The retained specimens had sufficient transverse reinforcement both within and outside potential plastic hinge regions to carry the maximum experimental shear developed during testing based on calculation, with the strengths established using the ATC-32 equations for shear strength (see Appendix for shear strength equations). Thus, the inelastic deformation capacity of the specimens was expected to be limited by mechanisms associated with flexural deformation rather than shear strength decay.

The retained data is used to observe effects of axial load ratio on experimentally-determined deformation capacities and as a basis for examining several proposed relations for estimating deformation capacity. The apparent displacement ductility, peak drift, and plastic rotation capacities of the specimens were examined using the identified ultimate displacements in conjunction with the estimated yield displacements and recommended values of plastic hinge length. The word "apparent" signifies data that was obtained or derived directly from the experiments. The ultimate displacements of the columns were determined by review of the measured response data. The ultimate displacement was defined as the maximum displacement corresponding to a 20% reduction of the maximum moment (including P-Δ contributions) developed during the experiment. This definition was used by Priestley [9] among others. Since this definition corresponds to a reduction in lateral strength, it may be assumed that vertical load carrying capacity was maintained throughout and beyond the ultimate displacement capacity as defined here. The use of a 20% drop is arbitrary and is intended to represent a substantial remaining flexural capacity for the confined concrete section.

The apparent peak drift capacities of the retained specimens are plotted in Figure 6 as a function axial load and confinement, expressed as percentage of the transverse reinforcement required by ATC-32. The numbers on the plot indicates the drift capacities whereas the "+" sign means that the test was stopped prematurely; additional drift capacity is available. The scatter at low and high axial load ratios is similar. The figure also shows that if 100 percent of ATC-32 transverse steel is provided, a drift capacity of 4.5% or more can be obtained for the entire range of $P/f_c'A_g$. Similarly, specimens with ATC-32 compliant transverse reinforcement achieved a displacement ductility capacity of 6 or more and a plastic rotation capacity of 0.04 or more, over the entire range of P/f'_cA_g (Inel [10]).

Table 2. Column test specimen parameters

Column ID[a]	Ref. #	f_c' MPa	B mm	H mm	M/VD[b]	cover[c] mm	f_y[d] MPa	ρ_l[e]	f_{yh}[f] MPa	s[g] mm	ρ_s[h]	$P/A_g f_c'$[i]
AN81-3	[11]	23.6	400	400	4.00	22.5	427	1.5%	320	100	2.94%	0.38
AN81-4	[11]	25.0	400	400	4.00	24.5	427	1.5%	280	90	2.30%	0.21
SO86-1	[12]	46.5	400	400	4.00	13.0	446	1.5%	364	85	0.86%	0.10
SO86-2	[12]	44.0	400	400	4.00	13.0	446	1.5%	360	78	1.22%	0.30
SO86-3	[12]	44.0	400	400	4.00	13.0	446	1.5%	364	91	0.80%	0.30
SO86-4	[12]	40.0	400	400	4.00	13.0	446	1.5%	255	94	0.57%	0.30
ZA86-7	[13]	28.3	400	400	4.00	13.0	440	1.5%	466	117	1.66%	0.23
ZA86-8	[13]	40.1	400	400	4.00	13.0	440	1.5%	466	92	2.12%	0.39
SA89-U6	[14]	37.3	350	350	2.86	26.1	437	3.3%	425	65	1.91%	0.13
SA89-U7	[14]	39.0	350	350	2.86	26.1	437	3.3%	425	65	1.91%	0.13
WA89-5	[15]	41.0	400	400	4.00	13.0	474	1.5%	372	81	1.18%	0.50
WA89-6	[15]	40.0	400	400	4.00	13.0	474	1.5%	388	96	0.56%	0.50
WA89-7	[15]	42.0	400	400	4.00	13.0	474	1.5%	308	96	2.21%	0.70
WA89-8	[15]	39.0	400	400	4.00	13.0	474	1.5%	372	77	1.24%	0.70
WA89-9	[15]	40.0	400	400	4.00	13.0	474	1.5%	308	52	4.08%	0.70
KH91-AS3	[16]	33.1	305	305	4.83	14.3	508	2.5%	508	108	1.57%	0.60
KH91-AS17	[16]	31.2	305	305	4.83	14.3	508	2.5%	508	108	1.57%	0.77
KH91-AS18	[16]	32.7	305	305	4.83	12.8	508	2.5%	464	108	2.65%	0.77
KH91-AS19	[16]	32.3	305	305	4.83	15.0	508	2.5%	489	108	1.12%	0.47
TA90-5	[17]	32.0	550	550	3.00	40.0	511	1.3%	325	110	1.71%	0.10
TA90-7	[17]	32.1	550	550	3.00	40.0	511	1.3%	325	90	2.08%	0.30
LI95-1	[18]	33.2	400	400	4.13	20.0	450	1.6%	362	70	2.07%	0.30
LI95-4	[18]	35.7	400	400	4.13	20.0	460	1.6%	362	55	2.63%	0.50

[a] column designation
[b] aspect ratio: M/V= shear span, and D = section depth
[c] cover= concrete clear cover, distance from outside to the confinement bar
[d] longitudinal reinforcement yield strength
[e] longitudinal reinforcement ratio
[f] transverse steel yield strength
[g] transverse reinforcement spacing
[h] volumetric transverse steel ratio
[i] axial load ratio: P= compressive axial load, A_g = gross area of cross section

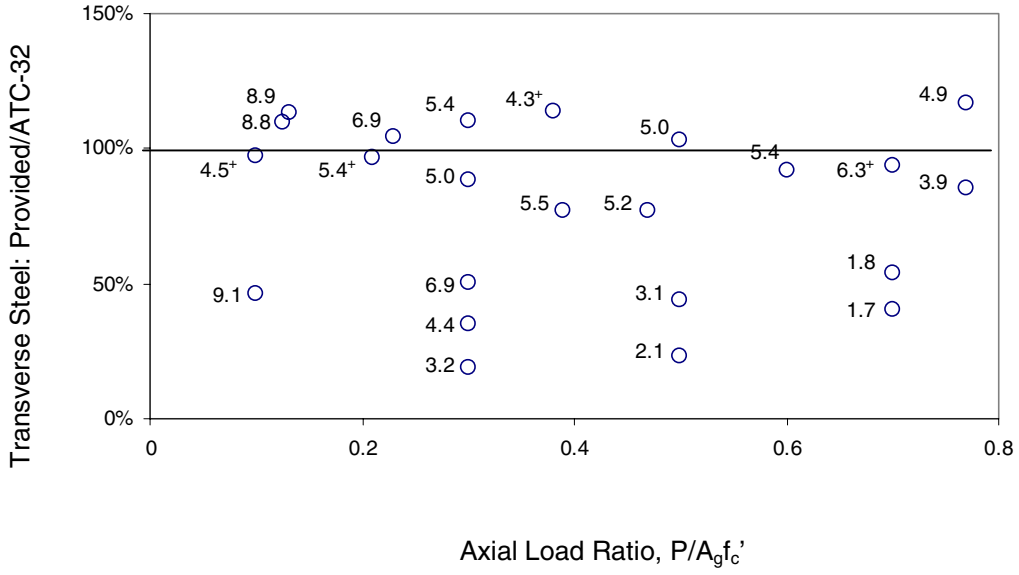

Figure 6. Apparent peak drift capacities of retained specimens as a function axial load and confinement, expressed as percentage of the transverse reinforcement required by ATC-32. The numbers on the figure indicate drift capacities (in percent) and the + sign means that the test was stopped prematurely to the loss of lateral capacity; additional drift capacity is available.

COMPARISON OF APPARENT AND ESTIMATED DEFORMATION CAPACITIES

The apparent inelastic deformation capacities relied upon Δ_y and L_p estimated using available models such as the "simple", Lehman, Fardis analytical, and Priestley models. These models would have to estimate values of apparent θ_p in order to accurately estimate the experimentally determined values of Δ_u. This section compares the apparent plastic hinge rotation capacity values with the estimates of θ_p according to the four models that use the lumped plasticity model. The Fardis empirical model is also considered for comparison purposes. For this model, the apparent plastic displacement $\Delta_{p,apparent}= \Delta_{u,apparent}-\theta_y L$ was compared to the estimated plastic displacement $\Delta_{p,estimated}= (\theta_{u,}-\theta_y)L$, where θ_y and θ_u were computed using the proposed equations of Fardis [5]. The purpose of the comparisons of this section is to illustrate the reliability of the apparent inelastic deformation capacities determined from the experimental data set, rather than showing the accuracy or inaccuracy of the models. The estimated plastic hinge rotation capacities of the models that use the lumped plasticity model were calculated as $\theta_p= (\phi_u- \phi_y)L_p$.

Comparison between the apparent and estimated deformation capacities underscores the differences among the five models. The ratio of the estimated and the apparent deformation capacities is plotted in Figure 7 against axial load ratio and transverse reinforcement content to identify possible trends. The figure shows that as axial load ratio increases the differences between models become more noticeable. One obvious reason is the differences in the equations for plastic hinge length calculation. The "simple", Fardis analytical, and Priestley models do not consider the axial load ratio in calculating the plastic hinge length while the Lehman model depends explicitly on the axial load ratio. The effect of transverse reinforcement on the plastic rotation capacity is considered further. As the percentage of ATC-32 transverse reinforcement increases, all models except the Fardis empirical model tend to estimate higher

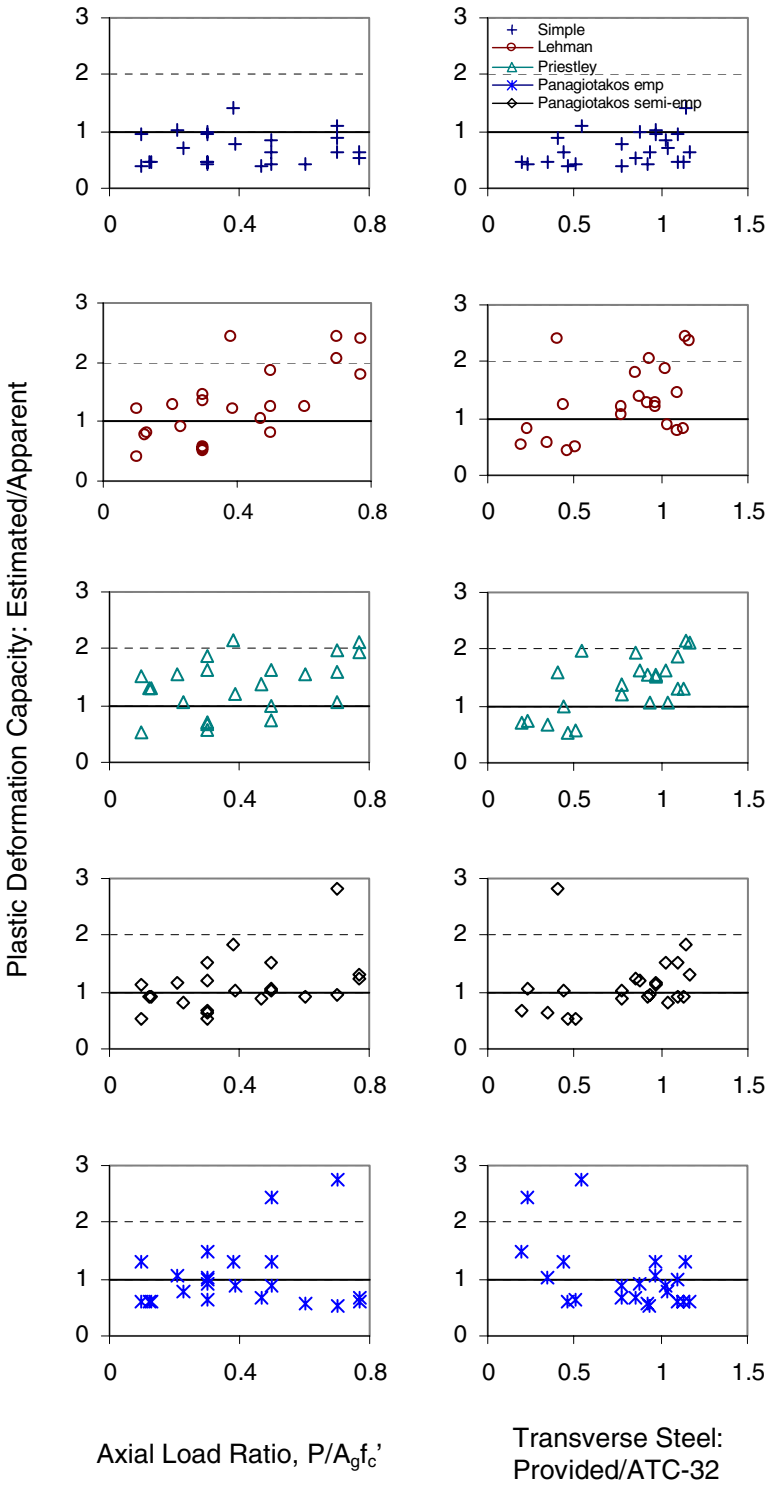

Figure 7. Ratio of the estimated to the apparent plastic deformation capacities of experimental data set vs. axial load ratio and transverse steel content.

capacities, indicating that the models exaggerate the effect of transverse steel on deformation capacity. The "simple" model tends to underestimate the plastic deformation capacity while the other models, especially the Lehman and Priestley models, can overestimate the plastic deformation capacity.

SUMMARY AND CONCLUSIONS

Five models for estimating the deformation capacities of members whose behavior is dominated by flexural deformations were reviewed in an attempt to characterize the model predictions and to establish the parametric sensitivity of various indices of deformation capacity (i.e. displacement ductility, plastic hinge rotation, and peak drift capacities). Because the deformation capacity models indicated a large range of expected deformation capacity and did not identify a single robust measure of inelastic deformation capacity, a limited set of experimental data obtained from tests of large-scale reinforced concrete columns having rectangular cross sections was investigated. Observations drawn from the deformation capacity models and the study of experimental data are summarized in this section.

Based on the parametric study of deformation capacity models, it is concluded that (a) no single deformation capacity index (e.g. plastic hinge rotation, drift, etc.) can be relied upon to give consistent estimates, as expected values vary with aspect ratio in a way that depends on the deformation capacity model; (b) plastic rotation capacity was not strongly dependent on axial load ratio when confinement was provided satisfying ATC-32 requirements; (c) the analytical models lead to large variations in deformation capacity estimates; (d) overall, the "simple" model tends to give lower bound estimates of deformation capacity, especially for plastic hinge rotation and drift capacities for columns with aspect ratios of 3 or greater; and (e) displacement ductility, plastic hinge rotation, and drift capacities (as percentage of specimen length) are independent of the absolute size (or scale) of the member for a given aspect ratio (minor differences relating to cover requirements and nominal bar diameters were neglected in the study).

Based on the evaluation of a limited set of experimental data, it is concluded that (a) the test specimens with ATC-32 compliant transverse reinforcement achieved a displacement ductility capacity of 6 or more, a plastic rotation capacity of 0.04 or more, and a drift capacity of 4.5% or more; (b) the scatter in the apparent deformation capacities is similar at low and high axial load ratios; (c) some of the analytical models can substantially overestimate the deformation capacities apparent in test data; and (d) some of the analytical models appear to exaggerate the effect of transverse steel on deformation capacity.

REFERENCES

1. Park R, Paulay T. Reinforced Concrete Structures, John Wiley & Son, Inc, New York, 769 pp, 1975.
2. Priestley MJN, Seible F, Calvi GMS. Seismic Design and Retrofit of Bridges, John Wiley & Sons, Inc., New York, 1996.
3. Lehman DE, Moehle JP. "Seismic performance of well-confined concrete bridge columns". Pacific Earthquake Engineering Research Center, Report No. PEER-1998/01, University of California, Berkeley, CA, USA, 1998.
4. Elwood KJ. "Shake Table Tests and Analytical Studies on the Gravity Load Collapse of Reinforced Concrete Frames". Ph.D. Thesis, University of California, Berkeley,CA, USA, 2002.
5. Fardis MN and Biskinis DE. "Deformation of RC members, as controlled by flexure or shear". Proceedings of the International Symposium Honoring Shunsuke Otani on Performance-Based Engineering for Earthquake Resistant Reinforced Concrete Structures, The University of Tokyo, Tokyo, Japan. September 8-9, 2003.

6. Panagiotakos TB, Fardis MN. “Deformation of reinforced concrete members at yielding and ultimate”. ACI Structural Journal, Vol. 98, No. 2, pp. 135-148, 2001.
7. ATC-32. “Improved seismic design criteria for California bridges: Provisional Recommendations”. Applied Technology Council, Redwood City, California, 1996.
8. Mander, JB, Priestley, M. J. N., and Park R. “Theoretical stress-strain model for confined concrete”. Journal of Structural Engineering, ASCE, Vol. 114, No. 8, pp. 1804-1825, 1988.
9. Priestley MJN and Park R. “Strength and ductility of bridge substructures”. Road Research Unit Bulletin #71, National Roads Board, Wellington, New Zealand, 1984.
10. Inel M. “Displacement-based strategies for the performance-based seismic design of short bridges considering embankment flexibility”. Ph.D. Thesis, University of Illinois at Urbana-Champaign, 2002.
11. Ang BG. “Ductility of Reinforced Concrete Bridge Piers under Seismic Loading”. Research Report 81-3, Department of Civil Engineering, University of Canterbury, Christchurch, New Zealand, February, 1981.
12. Soesianawati MT. “Limited Ductility Design of Reinforced Concrete Columns”. Research Report 86-10, Department of Civil Engineering, University of Canterbury, Christchurch, New Zealand, March 1986.
13. Zahn FA. “Design of Reinforced Concrete Bridge Columns for Strength and Ductility”. Research Report 86-7, Department of Civil Engineering, University of Canterbury, Christchurch, New Zealand, March 1986.
14. Saatcioglu M and Razvi SR. “Strength and Ductility of Confined Concrete”. Journal of Structural Engineering, ASCE, 1992, Vol. 118, No. 6, pp. 1590-1607.
15. Watson S. “Design of Reinforced Concrete Frames of Limited Ductility”. Research Report 89-4, Department of Civil Engineering, University of Canterbury, Christchurch, New Zealand, January 1989.
16. Khoury SS. “Behavior of Normal and High Strength Confined Concrete Columns With and Without Stubs”. Ph.D. Dissertation, University of Houston, December 1991.
17. Tanaka H. “Effect of Lateral Confining Reinforcement on the Ductile Behavior of Reinforced Concrete Columns”. Research Report 90-2, Department of Civil Engineering, University of Canterbury, Christchurch, New Zealand, June 1990.
18. Li Xinrong. “Reinforced Concrete Columns Under Seismic Lateral Force and Varying Axial Load”. Research Report 95-5, Department of Civil Engineering, University of Canterbury, Christchurch, New Zealand, August 1995.
19. ACI Committee 318. “Building Code Requirements for Structural Concrete (318-99) and Commentary (318R-99)”. American Concrete Institute, Farmington Hills, Michigan, 1999, 391 pp.
20. Caltrans BDS. “Bridge Design Specifications”. California Department of Transportation, 1995, Sacramento, California.

APPENDIX: ATC-32 TRANSVERSE STEEL REQUIREMENTS AND SHEAR STRENGTH

This Appendix summarizes the ATC-32 requirements for transverse reinforcement for rectangular reinforced concrete columns and shear strength equations.

There are differences among the provisions of various codes for the amount and distribution of column transverse reinforcement and calculation of shear strength (i.e. ACI Building Code [19] and Caltrans Bridge Design Specifications [20]). This study defines well-detailed as those that satisfy the ATC-32 [7] provisional recommendations for the detailing of longitudinal and transverse reinforcement. The focus here is on the confinement required in potential plastic hinge regions; requirements for other regions typically are somewhat relaxed and are not discussed here.

The recommended revisions to the Caltrans Specifications that are reported in ATC-32 require for potential plastic hinge regions:

$$A_{sh} \geq 0.12 s h_c \frac{f_{ce}^{'}}{f_{yhe}} \left(0.5 + 1.25 \frac{P}{A_g f_{ce}^{'}} \right) + 0.13 s h_c (\rho_l - 0.01) \quad \text{(A-1)}$$

where A_{sh}= total cross-sectional area of transverse reinforcement for a rectangular column in the direction perpendicular to the core dimension h_c, s= spacing of transverse reinforcement measured along the longitudinal axis of the column, h_c= cross-sectional dimension of column core measured center-to-center of confining reinforcement, A_g= gross area of the column, P= axial load on the column f_{ce}'= expected compressive strength of concrete, taken as $1.3f_c$' in ATC-32, f_{yhe}= expected yield strength of transverse reinforcement, taken as $1.1f_{yh}$ in ATC-32, and ρ_l= longitudinal reinforcement ratio of the column.

The calculation of shear strength per ATC-32 is summarized below.

$$V_c = \frac{1}{6} \left(1 + 0.075 \frac{P}{A_g} \right) \sqrt{f_c^{'}} b d \qquad (f_c^{'} \text{ in MPa}) \quad \text{outside of plastic hinge region} \quad \text{(A2)}$$

$$V_c = \frac{1}{6} \left(0.5 + 0.075 \frac{P}{A_g} \right) \sqrt{f_c^{'}} b d \quad (f_c^{'} \text{ in MPa}) \quad \text{in plastic hinge region} \quad \text{(A3)}$$

$$V_s = \frac{A_v f_{yh} d}{s} \quad \text{(A4)}$$

$$\phi V_n = \phi (V_c + V_s) \geq V_u \quad \text{(A5)}$$

where V_c= the nominal shear strength provided by the concrete, V_s= the nominal shear strength provided by the transverse reinforcement, V_u= the shear demand at the section considered (the maximum experimental shear developed during testing), f_c'= specified or reported compressive strength of concrete, A_v= the total area of the shear reinforcement parallel to the applied shear force with a spacing of s along the axis of the member, b= the width of the section, d= distance from extreme compression fiber to centroid of the longitudinal tension reinforcement, ϕ= strength reduction factor (taken as unity for the data set), and other terms are as defined previously.

The shear strength capacities within and outside potential plastic hinge regions of each specimen were calculated according to ATC-32 and the minimum value was taken as the calculated shear strength of each specimen. The shear demand was obtained from the experimental reports as $V_u = M_{max}/L$, where M_{max} is the maximum moment (including P-Δ contributions) developed during the experiment and L is the specimen height. Based on these calculations, all specimens have sufficient transverse reinforcement to carry the shear demands developed during testing. Therefore, the inelastic deformation capacity of the specimens would be expected to be limited by mechanisms associated with flexural deformation rather than shear strength decay.